

## Generation of Calibration Curves for the AWCC with Different NM Samples using the MCNP Code

W. El-Gammal<sup>1</sup>, A.G. Mostafa<sup>2\*</sup> and M. Ebied<sup>3</sup>

<sup>1</sup> Egyptian Nuclear and Radiological Regulatory Authority, Division of Regulations and Radiological Emergencies, Department of Nuclear Safeguards and Physical Protection, Nasr City, P.O. Code 11787, Cairo, Egypt

<sup>2</sup> Physics Department, Faculty of Science, Al-Azhar Univ., Nasr City, P.O. Code 11884, Cairo, Egypt

<sup>3</sup> Atomic Energy Authority, National Center for Radiation Research and Technology, Division of Industrial Irradiation, Department of Nuclear Safety Research and Radiation Emergency, Nasr City, P.O. Code 11762, Cairo, Egypt

\*[drahmedgamal@yahoo.com](mailto:drahmedgamal@yahoo.com)

**Abstract:** This paper aims to generate calibration curves for different nuclear material samples to be measured in the Active Well Neutron Coincidence Counter (AWCC). The curves are generated using the MCNP code to relate the real coincidence count rates with <sup>235</sup>U mass contents in samples. This approach will reduce both the measurement effort and the heavy reliance on unavailable or expensive reference materials required for calibrating the instrument. The real coincidence count rates for different nuclear material shapes, compositions, densities and <sup>235</sup>U enrichment are calculated.

[El-Gammal W, Mostafa AG and Ebied M. **Generation of Calibration Curves for the AWCC with Different NM Samples using the MCNP Code.** *Nat Sci* 2015;13(8):111-116]. (ISSN: 1545-0740).

<http://www.sciencepub.net/nature>. 18

**Keywords:** Nuclear Safeguards; Monte Carlo; Detector calibration; Uranium; AWCC; NDA

### 1. Introduction

The AWCC is a neutron coincidence counting system that could be operated in either active or passive counting modes [1]. It is a transportable high-efficiency counter for measuring uranium isotopic masses in uranium bearing materials. The active mode operation of the AWCC is based on the detection of coincidence neutrons produced from induced fission of <sup>235</sup>U isotope using interrogation neutron sources (one or more Am-Li neutron sources are inserted in the top and/or bottom of the detector well). The construction of AWCC, its associated electronic units and the method of operation were described and explained by many authors in various papers and technical reports [1-5].

The relationship between the response of the AWCC system and the fissile mass of the sample is commonly expressed in the form of a calibration curve (<sup>235</sup>U mass versus coincidence counts). This calibration normally performed through measuring standard nuclear material (SNM) samples. Because of neutron absorption and multiplication in uranium samples, the calibration curves are nonlinear, sensitive to the NM geometry and density and other factors. Therefore, to obtain accurate quantitative measurements using AWCC, it is necessary to calibrate the instrument using physical standards representative of the unknown sample under investigation.

However, an appropriate calibration curve is not always available, either because suitable standards are expensive and not available or it is

difficult to obtain the large number of physical standards necessary for accurate assaying of the wide categories and shapes of NM [6, 7].

The AWCC was tested and used in different applications by many authors [7-13]. They showed that the instrument could be used for assaying wide range of High and Low enriched uranium samples in different forms and shapes, either in thermal or fast modes taking into consideration the neutron self-shielding and multiplication. It has been demonstrated that AWCC can be applied for assaying uranium content in wide variety of materials, masses and matrix impurities in addition to the generation of calibration curves for different NM categories using the relevant suitable SNM. Different application using cross-calibration investigation for AWCC were also considered [12- 13].

Many authors tried to model AWCC using Monte Carlo code. Rinard and Menlove [14] used the MCNP-REN code to model the AWCC in a configuration used to measure uranium linear density in long fuel elements. The simulation results showed about 10% positive bias. Pozzi et al [15] used MCNP-PoliMi code to simulate the measurements performed with AWCC via simulating the operation of the counter shift register. They showed that the calculated efficiency for the AWCC using Cf-252 is 29% while in case of induced fission neutron detection, the efficiency reduced to be 25.6% using 6.0 kg of uranium metal with enrichment equal to 92.0% and AmLi neutron sources in their positions.

In most of the reviewed work, it was noticed that, to obtain accurate quantitative measurements, it is necessary to calibrate the instrument using physical standards representing the samples to be assayed. Hence a model for AWCC calibration is proposed to overcome the difficulties in providing the suitable SNM. The model employs the general Monte Carlo simulation code.

## 2. Methodology

In a previous work [16], it was shown that the relation between the detected coincidence count rate of fission neutrons ( $Cr_5$ ) and the measured  $^{235}\text{U}$  mass ( $M_5$ ) could be given as:

$$Cr_5 = M_5 F_5 f_{c5} \quad (1)$$

Where:

$F_5$  is the total specific fission rate of  $^{235}\text{U}$  isotope (fissions/s.g).

$f_{c5}$  is the counter coincidence counting efficiency due to the fission neutrons of  $^{235}\text{U}$  isotope.

The fission rate depends on many parameters such as the neutron spectrum of the interrogation source, characteristics and setting up configuration of the counter as well as the characteristics of the measured sample [17-20].

To avoid estimating the effect of such parameters and to overcome the lack of NM standards, a model has been suggested to calibrate the detector mathematically. A full mathematical calibration of the AWCC will take into account the fission rate and counter efficiency indicated in Equation (1). For a uranium-bearing sample assayed in the AWCC, the coincidence count rate could be given as:

$$C_{r5} = \left( \frac{S_T - S_o}{v_T} \right) \cdot \left( 1 - \frac{S_f}{f_i} \right) \quad (2)$$

Where:

$S_T$  is the total singles count rate ( $\text{s}^{-1}$ ), estimated using MC calculations.

$S_o$  is the total singles count rate ( $\text{s}^{-1}$ ) due to all interactions but fission, estimated using MC calculations for samples free of any NM.

$S_f$  is the singles count rate for fission neutrons with  $v=1$  ( $\text{s}^{-1}$ ).

$S_f/f_i$  is the fraction of the fission neutrons (with  $v=1$ ) to the total fission neutrons (it could be deduced from induced fission multiplicity table from the MCNPX output file).

$v_T$  is the total neutron multiplicity for the mean value of neutrons emitted per spontaneous or induced fission (it could be deduced from induced fission multiplicity table from the

MCNPX output file for every correspondence single or couple measured samples).

Equation (2) shows that for a certain  $^{235}\text{U}$  bearing sample,  $C_{r5}$  could be estimated using MC calculations. By assuming different  $^{235}\text{U}$  mass contents, different corresponding count rates could be estimated, and hence, a calibration curve could be constructed.

## 3. Monte Carlo Modeling for AWCC

The complete MCNP model of the AWCC system was described previously [16]. The detector was modeled in the vertical configuration, active thermal mode, with 27.54 cm cavity height and 22.86 cm diameter. The AmLi sources were placed at their positions in lower and lid plugs, at 10.72 and 42.74 cm from the bottom of the detector to allow optimum sample interrogation, Fig. (1). The counter dimensions, its components, their locations, effective lengths, densities, material properties of  $^3\text{He}$  and AmLi sources yields and directions were obtained or calculated according to the available data given in different references [4, 5, 21, 22, 23, 24 & 25]. The ideal  $^{241}\text{AmLi}$  neutron source energy spectrum, in a numerical format used in the simulation process was calculated by Tagziria and Looman [26].

In this work, uranium in different masses, chemical compounds, densities, enrichments and shapes were assumed to generate (mathematically) different calibration curves for the AWCC using the MCNP5 general MC code.

### Uranium mass

A wide range of  $^{235}\text{U}$  masses varied from 10.0 up to 100.0 g content in the form of  $\text{U}_3\text{O}_8$  was assumed. MC calculations for this range of masses were performed at constant enrichment of 3.0% and material density of  $4.0 \text{ g/cm}^3$ . The NM located in the center of the cavity in a cylindrical shape without any container to avoid any effects from any other factors. By increasing the mass of NM, the volume increases accordingly. This increase in volume was treated in two different ways:

- The height of the NM was varied gradually from 1.25 to 12.5 cm, while the radius was kept constant ( $r = 5.0 \text{ cm}$ ),
- The radius of the NM was varied gradually from 2.5 to 7.79 cm, while the height was kept constant ( $h = 5.0 \text{ cm}$ ).

The effect of material composition was studied by considering the same calculations for  $\text{UO}_2$  instead of  $\text{U}_3\text{O}_8$  except for the variation in NM height (from 1.2 to 12.04 cm at constant radius of 5.0 cm).

### NM Density

A mass of 100 g of  $^{235}\text{U}$  content (in the form of  $\text{U}_3\text{O}_8$ ) with 3.0 % enrichment were modeled with NM densities varied from 2.0 to  $10.0 \text{ g/cm}^3$ . The

height of the material was kept constant (10.0 cm) while its radius was varied from 7.91 to 3.54 cm with increasing density.

Also, the real coincidence count rates were calculated for different NM sample ( $\text{UO}_2$ ) densities.

The calculations were performed for sample densities of 4.0 and 10.97  $\text{g}/\text{cm}^3$  (which is common for some nuclear reactor fuel).

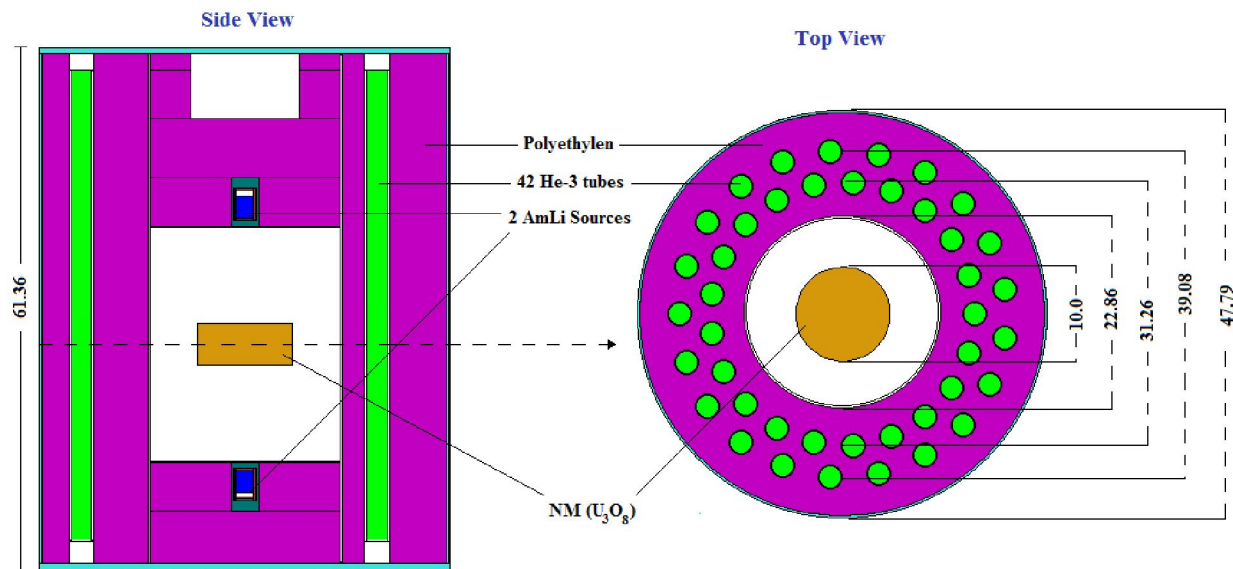


Figure 1. MCNP5 model of a Canberra JCC-51 Active Well Coincidence Counter.

### Uranium Enrichment

The effect of enrichment changes was studied by modeling samples with constant mass (100 g) of  $^{235}\text{U}$  in  $\text{U}_3\text{O}_8$  samples with 4.0  $\text{g}/\text{cm}^3$  density and with enrichment varied between 3.0% and 19.9%. Different enrichment values were considered via changing the amount of  $^{238}\text{U}$  and  $^{234}\text{U}$  in the samples. In the current case the radius of the material was chosen to be constant at 5.0 cm, while the height varies from 12.5 to 20.85 cm as the enrichment is increased.

### NM shape

100 g of  $^{235}\text{U}$  content in  $\text{U}_3\text{O}_8$  with density 4.0  $\text{g}/\text{cm}^3$  and enrichment 3.0 % have been modeled in six geometrical shapes. The assumed shapes are sphere ( $r = 6.167$  cm), cylinder ( $h = 6.256$  cm,  $r = 7.07$  cm), cylinder ( $h = 12.512$  cm,  $r = 5.0$  cm), rectangular ( $h = 15.782$  cm,  $l = 7.891$  cm,  $w = 7.891$  cm) cube ( $h = 9.942$  cm) and spherical shell ( $r_{\text{in}} = 8.439$  cm,  $r_{\text{out}} = 9.419$  cm).

## 4. Results and Discussion

MCNP simulation model for AWCC has been used to generate different calibration curves for the detector using NM samples in different conditions

This effect is not clear here and there is no large difference, as the percentage of oxygen mass weight in the above mentioned compounds are

and shapes that are expensive or even difficult to be created and measured directly as follows:

### a. Uranium mass

Fig. (2) illustrates the calculated real coincidence count rate for a wide range of  $^{235}\text{U}$  masses (varies from 10.0 to 100.0 g) in a cylindrical shape varies as follows:

- The height of NM varies while the radius stays constant at 5.0 cm.
- The radius of NM varies while the height stays constant at 5 cm.

Both the two curves indicate that the coincidence count rate increase with increasing the surface area exposed to the neutron yields from the two AmLi interrogation sources. The effect of the shape will be discussed more in this paper later.

Fig. 3 illustrates a comparison between  $\text{U}_3\text{O}_8$  and  $\text{UO}_2$  calculated real coincidence count rate for a wide range of  $^{235}\text{U}$  masses. The difference in coincidence count rates for both of the two compounds is found to be so small and the largest change is less than 1.9% for the sample with 50 g  $^{235}\text{U}$  mass.

Oxygen bounded with the fissile element affects neutron transportation through the compound; hence it affects fission and coincidence count rates. approximately close (15.2% and 11.85% for  $\text{U}_3\text{O}_8$  and  $\text{UO}_2$  respectively). Although the effects of

oxygen compounds are close, they should not be ignored and have to be taken into consideration [27].

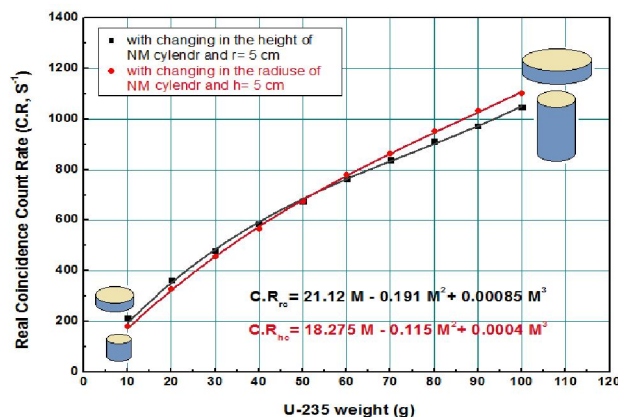


Figure 2. The calculated real coincidence count rate for a wide range of <sup>235</sup>U masses content in U<sub>3</sub>O<sub>8</sub> in a cylindrical shape.

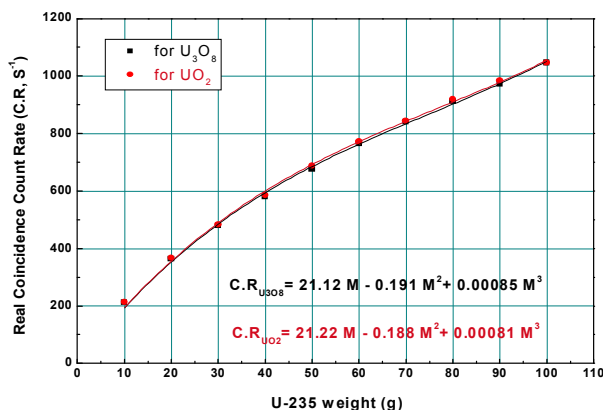


Figure 3. Comparison between U<sub>3</sub>O<sub>8</sub> and UO<sub>2</sub> calculated real coincidence count rate for a wide range of <sup>235</sup>U masses.

**b. NM Density**

To examine the effect of density on the coincidence count rate, 100 g of <sup>235</sup>U content in U<sub>3</sub>O<sub>8</sub> with 3.0 % enrichment and density varies from 2.0 to 10 g/cm<sup>3</sup> have been modeled in cylindrical shape with height of 10.0 cm. Fig. (4) shows that the coincidence count rate decreases exponentially by increasing the density and there is about 37.0 % drop in the calculated result over such large density range.

The comparison of the coincidence count rate for UO<sub>2</sub> with two specific densities (4.0 and 10.97 g/cm<sup>3</sup>) along <sup>235</sup>U different masses varies from 10.0 to 100.0 g has been illustrated in Fig. (5). It shows that the difference increases gradually by increasing the NM mass (from 4.22 % at 10 g to become 22.03 % at 100 g). This is because the effect of uranium self-screening increases by increasing the density for large masses with very thick blocks. It

leads also to a decrease in the fraction of thermal neutron absorbed by <sup>235</sup>U to make fission or even the fraction of the fission neutrons leaving the NM.

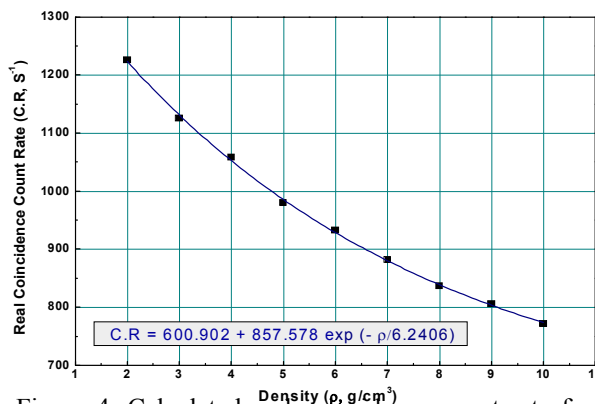


Figure 4. Calculated real coincidence count rate for 100 g of <sup>235</sup>U content in U<sub>3</sub>O<sub>8</sub> (3.0% enriched) as a function of density.

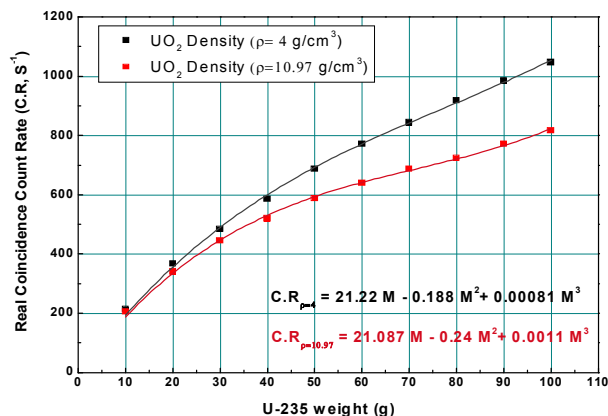


Figure 5. Calculated real coincidence count rate for a wide range of <sup>235</sup>U mass content in UO<sub>2</sub> (3.0% enriched) with two different densities.

**c. Uranium Enrichment**

A 100 g of <sup>235</sup>U content in U<sub>3</sub>O<sub>8</sub> with density 4.0 g/cm<sup>3</sup> and enrichment value varies from 3.0% to 19.9% has been modeled to investigate the effect of changing the enrichment. The enrichment was changed by adjusting the amount of <sup>238</sup>U and <sup>234</sup>U present. The results illustrated in Fig. 6 shows that the coincidence count rate decreases exponentially by increasing the enrichment and there is about 22.0 % drop in the count rate over the enrichment range from 3.0 to 19.9%. This decrease may be resulting from the decrease of <sup>235</sup>U surface area exposed to interrogating neutrons by increasing the enrichment (taking into account that; <sup>235</sup>U mass is constant to be 100 g for all samples with changing the masses of <sup>238</sup>U and <sup>234</sup>U to change the enrichment). Another reason for this decrease may be that by decreasing the enrichment the volume will increase and hence a

percentage of  $^{235}\text{U}$  atoms will be closer to the two AmLi sources.

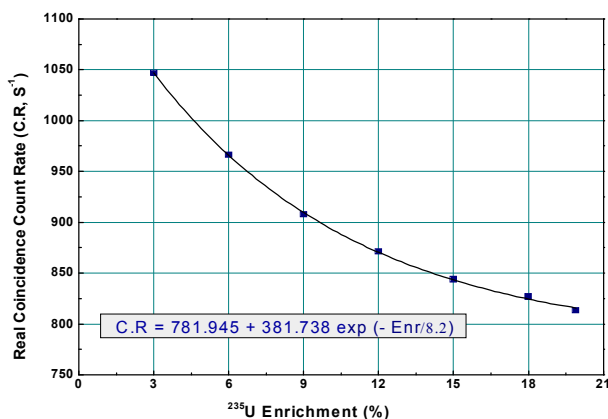


Figure 6. Calculated real coincidence count rate as a function of  $^{235}\text{U}$  enrichments ( $^{235}\text{U}$  mass is 100 g while the enrichment changes by changing the amount of  $^{238}\text{U}$  and  $^{234}\text{U}$ ).

#### d. NM shape

Six geometrical shapes for the same mass of  $^{235}\text{U}$  (100 g) content in  $\text{U}_3\text{O}_8$  with constant density of  $4.0 \text{ g/cm}^3$  and 3.0 % enrichment have been modeled to compare the effect of shape on the fission rate. Fig. (7) shows the coincidence count rate for sphere, cylinder ( $h = 2D$ ), rectangular, cube, cylinder ( $h = D$ ) and spherical shell respectively. It can be seen that the count rate increases by increasing the surface area exposed to the neutron yields (the sphere shape has the smallest surface area). A larger-diameter shape will have a smaller fill height for the same mass; hence the self-shielding will be reduced by spreading the material into a thinner shape and increase the probability that delayed neutrons will escape and go into the NM to react with  $^{235}\text{U}$ . The spherical shell can give a count rate higher than that from a solid sphere by about 18.8 % (of course this difference depends on the thickness of the shell). The coincidence count rate for other shapes will give results in-between.

#### 5. Conclusion

A mathematical calibration method using Monte Carlo simulation for  $^{235}\text{U}$  mass calibration in different shapes and conditions of the AWCC has been proposed. Using this model, it is easy to simulate calibration curves for the AWCC using NM with properties and characteristics that would be difficult and expensive to accomplish with physical standards.

A simple view has been given for the anticipated coincidence count rate of  $^{235}\text{U}$  in different masses, chemical compounds, densities, enrichments

and shapes within the cavity of the AWCC. It may help in giving a preliminary prediction for the effect of changing any of these parameters or the limitations of error for accurate determination of these parameters.

The data given in this paper are still necessary to be proven practically and more investigation is still needed to verify the validity of the model and the accuracy of the obtained calibration curves.

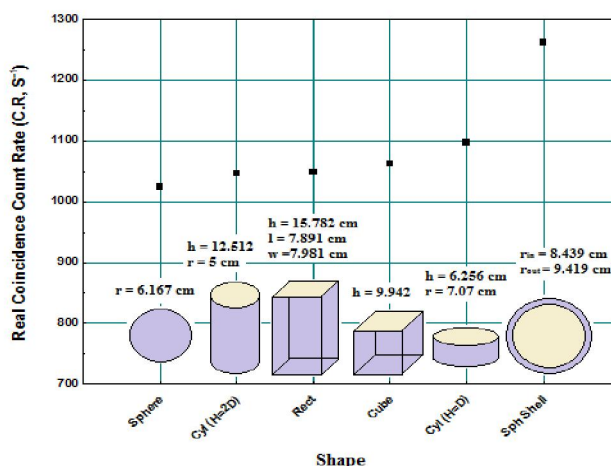


Figure 7. The Calculated real coincidence count rate for 100 g of  $^{235}\text{U}$  content in  $\text{U}_3\text{O}_8$  (3.0% enriched) with density  $4.0 \text{ g/cm}^3$  for different shapes

#### Corresponding Author:

Prof. Dr. Ahmed G. Mostafa  
Physics Department  
Faculty of Science  
Al-Azhar Univ., Nasr City, Cairo, Egypt  
E-mail: [drahmedgamal@yahoo.com](mailto:drahmedgamal@yahoo.com)

#### References

1. Model JCC-51 Active Well Neutron Coincidence Counter, Technical Paper, Canberra Industries, available on [http://www.canberra.com/products/waste\\_safeguard\\_systems/pdf/JCC-51-SS-C36907.pdf](http://www.canberra.com/products/waste_safeguard_systems/pdf/JCC-51-SS-C36907.pdf).
2. W. El-Gammal W. I. Zidan and E. Elhakim, A proposed semi-empirical method for  $^{235}\text{U}$  mass calibration of the Active Well Neutron Coincidence Counter, Nuclear Instruments and Methods (A), 565 (2006) 731.
3. H. O. Menlove, Description and operation manual for the Active Well Neutron Coincidence Counter, LA-7823-M, Los Alamos (1979).
4. H. O. Menlove and J. E. Swansen, Nucl. Technol., 71 (1985) 497.

5. J. E. Swansen, P. R. Collinsworth and M. S. Krick, Nuclear Instruments and Methods, (1980) 555.
6. M. S. Krick, N. Ensslin, D. G. Langner, M. C. Miller, R. Siebelist, and J. E. Stewart, Active Neutron Multiplicity Analysis and Monte Carlo Calculations, Institute of Nuclear Materials Management (INMM) Annual Meeting, Florida, USA, July 17-20, (1994).
7. H.O. Menlove and J. E. Stewart, A new method of calibration and normalization for neutron detector families, LA-11229-MS, Los Alamos (1988).
8. H. O. Menlove and G. E. Bosler, Application of the Active Well Coincidence Counter (AWCC) to high-enrichment uranium metal, LA-8621-MS, Los Alamos (1981).
9. M. S. Krick, H. O. Menlove, J. Zick and P. Ikonomou, Measurement of enriched uranium and uranium-aluminum fuel materials with the AWCC, LA-10382-MS, Los Alamos (1985).
10. J. K. Hartwell and G. D. McLaughlin, Non-destructive analysis of impure HEU-carbon samples using an Active Well Coincidence Counter (AWCC) 39, in: INMM Annual Meeting, Naples, FL, USA, 26–30, July (1998).
11. V. Mykhaylov, M. Odeychuk, V. Tovkanetz, V. Lapshyn, K. Thompson and J. Leicman, Use of AWCC in evaluation of unknown fissile materials: Symposium on International Safeguards, Verification and Nuclear Material Security, IAEA-SM-367, Vienna, Austria, 29 October - 2 November (2001).
12. B. A. Jensen, J. Sanders, T. Wenz and R. Buchheit, Results of Active Well Coincidence Counter cross-calibration measurements at Argonne National Laboratory-West, ANL-02/35, Argonne (2002).
13. H. O. Menlove, R. Siebelist and T. R. Wenz, Calibration and performance testing of the IAEA for Active Well Coincidence Counter (Unit 1), LA-13073-MS, Los Alamos (1996).
14. P. Rinard and H. O. Menlove, Monte Carlo simulations of an AWCC with long fuel assemblies, in: Symposium on Safeguards and Nuclear Material Management, Seville, Spain, 4–5 May (1999).
15. Sara A. Pozzi, Richard B. Oberer, and Lisa G. Chiang, Monte Carlo Simulation of Measurements with an Active Well Coincidence Counter, Oak Ridge National Laboratory available on <http://www.ornl.gov/~webworks/cppr/y2001/pres/120718.pdf>
16. W. El-Gammal, A. G. Mostafa and M. Ebied, On the Mathematical Calibration of the Active Well Neutron Coincidence Counter, accepted for publication in the American Journal of Physics and Application.
17. T. D. Reilly, N. Ensslin, H. A. Smith and S. Kreiner, "Passive Nondestructive Assay of Nuclear Materials," NUREG/CR-5550, LA-UR-90-732, Los Alamos National Laboratory, USA (1991).
18. N. Ensslin, W. C. Harker, M. S. Krick, D. G. Langner, M. M. Pickrell and J. E. Stewart, Application Guide to neutron multiplicity counting, LA-13422-M, Los Alamos (1998).
19. D. I. Garber and R. R. Kinsey, Neutron Cross Sections Curves, vol. II, Brookhaven National Laboratory (1976) 325.
20. M. Ebied, M. Sc Thesis, Investigation of Depleted Uranium Assay using Active Well Neutron Coincidence Counter, Physics Department, Faculty of Science, Al-Azhar University, April (2009).
21. CANBERRA, Model JCC-51, Active Well Neutron Coincidence Counter, User's Manual, USA (1998).
22. CANBERRA, Neutron Coincidence Counter checklist, <sup>3</sup>He Tube Data Sheets, USA (1998).
23. CANBERRA, Model JSR-14, Neutron analysis shift register, User's Manual, USA (1997).
24. Eric Chandler Miller, Characterization of Fissionable Material using a Time-Related Pulse-Height Technique for Liquid Scintillators, Ph.D., Nuclear Engineering and Radiological Sciences, University of Michigan (2012).
25. Corey Freeman, William Geist and Martyn Swinhoe, MCNPX Calculations of MTR Fuel Elements Measured in an Active Well Coincidence Counter, LA-UR-09-03916, Los Alamos, June (2009).
26. H. Tagziria and M. Looman, The ideal neutron energy spectrum of <sup>241</sup>AmLi ( $\alpha$ , n) 10B sources, Applied Radiation and Isotopes, 70 (2012) 2395.
27. Phillip M. Rinard, calculating accurate shuffler count rates with applications, LA-UR-01-2685, Los Alamos National Laboratory, INMM 42nd Annual Meeting, July (2001).